Multi-band, highly absorbing, microwave metamaterial structures

**T. M. Kollatou · A. I. Dimitriadis · S. D. Assimonis ·
N. V. Kantartzis · C. S. Antonopoulos**

Abstract A further example of multi-band absorption using ultra-thin, polarization-insensitive, wide-angled metamaterial absorbers that operate in multi-frequency bands within the microwave regime is presented in this work. The basic structure geometry is utilised to create multi-band highly absorbing structures by incorporating the scalability property of the metamaterials. Simulation results verify the structure's ability for high absorption. The multi-band absorbers are promising candidates as absorbing elements in scientific and technical applications because of its multi-band absorption, polarization insensitivity, and wide-angle response. Finally, the current distributions for those structures are presented to gain a better insight into the physics behind the multiple absorption mechanism.

1 Introduction

Metamaterials have been effectively used to produce highly absorbing structures which led the microwave engineers to research a new scientific field, with a direct impact on modern microwave systems. Since metamaterial absorbers are thinner than the traditional microwave absorbers, due to diffraction limit restrictions, they are perfect candidates to replace them as absorbing elements in scientific and technical applications. Essentially, metamaterials are inherently inhomogeneous structures, usually fabricated from metallic particles embedded in a host dielectric medium, and their properties mainly arise from the geometric details rather than their constituting material properties. A partic-

ular field in the metamaterial scientific territory, the metamaterial perfect absorber (MPA), has gained much interest due to its ability to achieve unity absorptivity of electromagnetic waves [1]. Since its first experimental verification in 2008, a considerable variety of metamaterial structures have been proposed to produce almost perfect absorption in the microwave, terahertz, and infrared frequency regions [2–5]. The interest for studying MPAs mainly arises from their use in potential applications. These applications include emitters, sensors, spatial light modulators, IR camouflage, thermophotovoltaics and wireless communication. Since there is still need for improvement of their performance, a lot of research is carried out to produce a wide range of incident angles and bandwidth-enhanced frequency spectrum [6–10]. This is a subject of huge importance for various electromagnetic interference/electromagnetic compatibility (EMI/EMC) problems.

The purpose of this paper is to present a further example of multi-band absorption, utilizing a family of ultrathin, polarization-insensitive, metamaterial structures with wide angles of incidence that can achieve high absorption in multiple frequencies within the microwave regime. This work is focusing on the various cases of oblique incidence for single-, double- and triple-band absorption and explanation of the physical mechanism behind the absorption, following the in-depth work that has been done previously in [11]. Having acquired the optimized unit-cell dimensions for an absorber operating in 8.2–12.4 GHz, we proceed to the design of multi-band absorbers. They are designed in a form of a supercell of several-different sized structures of square electric ring resonators (S-ERRs) [12] and a full metal back plate separated by a 1 mm thick FR-4 dielectric substrate, resulting in an electrically thin structure. The absorbing capability of the proposed family of absorbers is directly resulted from the resonant structures of the unit cell. Through simply scal-

T. M. Kollatou (✉) · A. I. Dimitriadis · S. D. Assimonis ·
N. V. Kantartzis · C. S. Antonopoulos
Department of Electrical and Computer Engineering,
Aristotle University of Thessaloniki, 54124 Thessaloniki, Greece
e-mail: fanikollatou@gmail.com

ing up and down the dimensions of the original S-ERR, it is possible to tune the absorbing frequency over a significant electromagnetic frequency spectrum.

2 Absorber characteristics

Absorbers are incorporated in various applications to eliminate unwanted scattering electromagnetic energy. For metamaterial absorbers, the most important parameter is the absorptivity, which is interpreted as the percentage of incident energy absorbed by the material. By minimizing the reflection and transmission of the incident radiation, we are able to design a reliable metamaterial absorber. By exploiting the definition of the absorption, utilizing the S-parameters, $A(\omega) = 1 - R(\omega) - T(\omega)$, with $(\omega) = |S11|2$ and $(\omega) = |S21|^2$ being the reflectance and transmittance, respectively.

Following the theoretical analysis, the basic structure of an efficient metamaterial absorber, which will be the fundamental component for the construction of our multi-band structures, is realized by imprinting a S-ERR at the front layer of a 1-mm thick FR- 4 dielectric substrate with a relative permittivity $\varepsilon_r = 4.1$ and loss $\tan \delta = 0.025$ (at 10 GHz) as in Fig. 1a. Note that the substrate is very thin and lightweight and determines the overall design's characterization as ultrathin (the thickness is $\lambda_0 = 30$ at the resonance frequency). The bottom layer is a full copper plane that guarantees zero transmission through the slab and is designed such that the incident magnetic field drives circulating currents between the two layers. The metallic parts are made of copper, which behaves as a perfect electric conductor (PEC) at the microwave spectrum. The unit-cell dimension and periodicity are around $\lambda/4$, hence, the final periodic absorber structure could not be considered as homogeneous. However, according to Fig. 2, it is observed that the induced charges accumulate mainly at the two edges of the squared unit-cell, and hence response to the incident electric field component. Similarly, according to Fig. 3, the induced currents are antiparallels, which response to the incident magnetic field component. Consequently, the physical mechanism responsible for the absorption ability of the periodical structure is similar with the metamaterial mechanism. The specific S-ERR has been chosen due to its fourfold rotational symmetry around z-axis .An array of infinite unit cells is formed by applying periodic boundary conditions along the x- and y-axis. All simulations are carried out using the conventional 3D finite difference method in time domain (3D-FDTD) [13]. The absorption peak [11] of 95.8 % occurs at the frequency of 10.3 GHz, while the reflectance is minimized at the same frequency.

The wide-angle performance of the proposed structure is tested and verified in Fig. 4 where high absorption curves, centered almost at the same frequency as the one referring

(a) (front view)   **(b) (side view)**
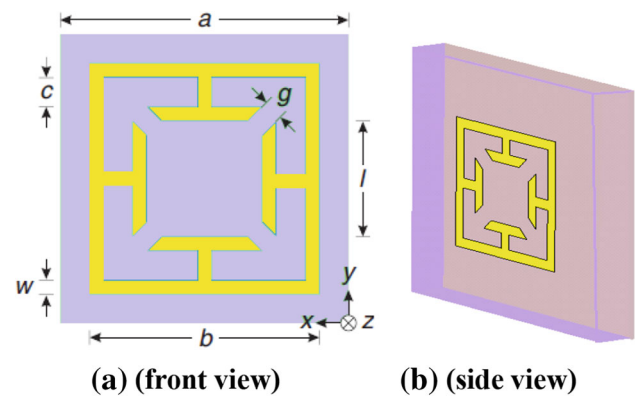
Fig. 1 Optimized unit cell (*square structure*) with $\alpha = 8$ mm, $b = 4.2$ mm, $c = 0.5$ mm, $l = 1.9$ mm, $g = 0.56$ mm, and $w = 0.32$ mm. Thickness of the copper layer (*yellow color*) is 35 μm, while the thickness of the substrate (*purple color*) is 1 mm


(a) (top layer)   **(b) bottom layer**
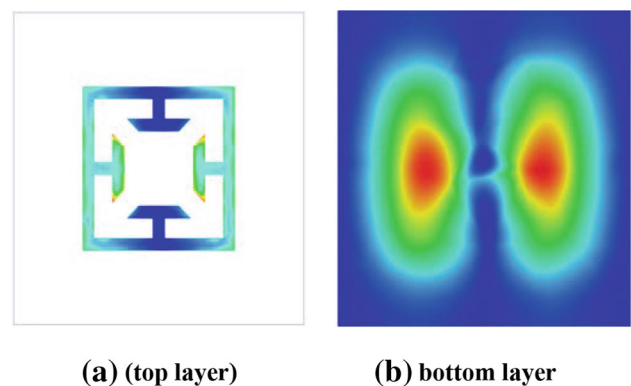
Fig. 2 The induced charges accumulate mainly at the two edges of the squared unit-cell and response to the incident electric field component

**(a) (top layer)**   **(b) (bottom layer)**
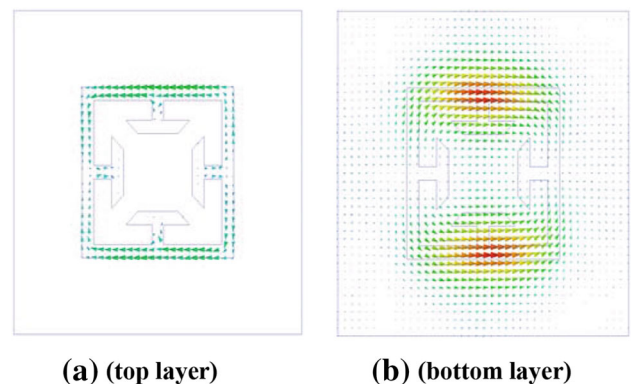
Fig. 3 The current distribution results in anti-parallel currents, response to the incident magnetic field

to normal incidence, are acquired even for large angles of incidence. In the first case, the electric field component is parallel to the x-axis and we vary the angle theta (θ) between the wavevector and the z-axis on the yz-plane. In the second case, we keep the magnetic field component parallel to the y-axis and modify the angle phi (φ) between the wavevector and the z-axis on the xz-plane as can be seen in Fig. 5. These two
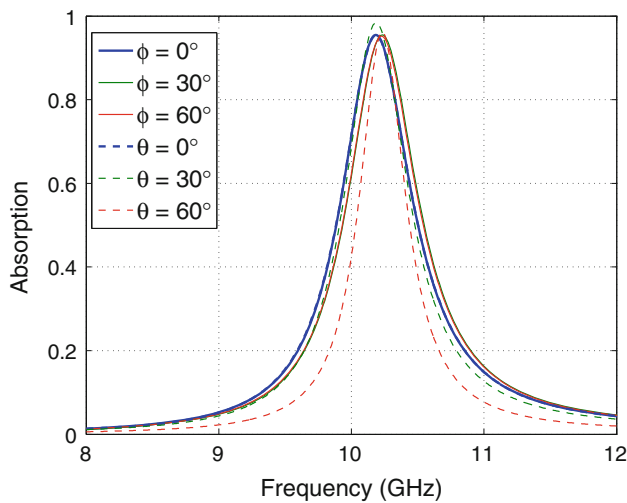
Fig. 4 Absorption efficiency of the proposed device for obliquely incident waves for two different cases
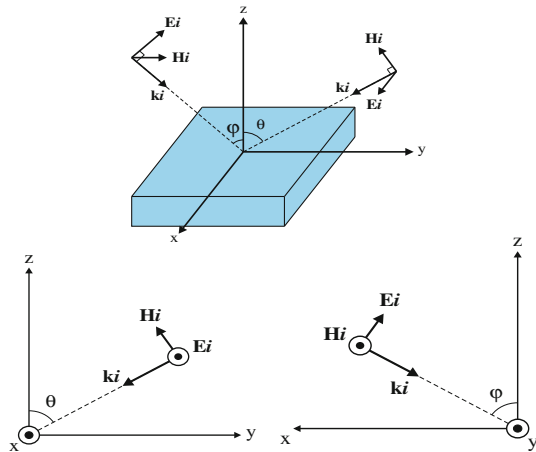

Fig. 5 Angles φ and θ for the cases of oblique incidence

cases could be considered to be equivalent to the propagation of TE- and TM-polarized plane waves, due to the absorber's four-folding symmetry around z.

Finally, an interesting observation points out how sensitive the structure is to changes of the substrate's dielectric properties. When the electric permittivity of the dielectric fluctuates from $\varepsilon_r = 4$ to $\varepsilon_r = 4.3$, the geometric features of the absorption curve remain unchanged, whereas the center frequency is shifted slowly up and down, as can be pointed out in Fig. 6. Depending on the application's operating frequency, a small change in the dielectric properties of the substrate can significantly influence the accuracy of the results (Table 1).

3 Towards multi-band absorption

Designing an absorber that operates efficiently in the desired frequency band, for oblique incident waves is of major impor-
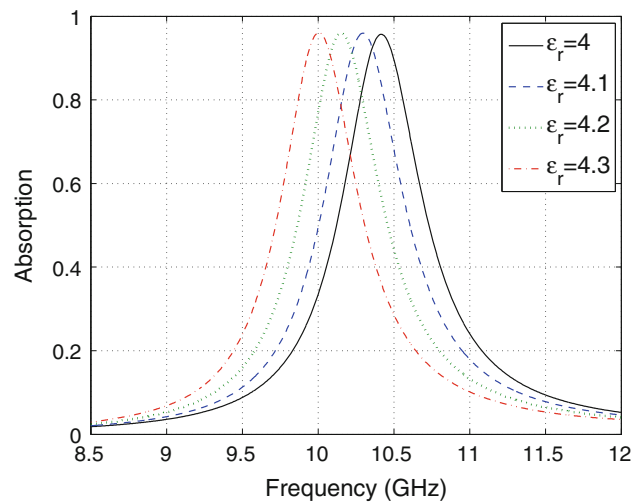
**Fig. 6** Absorption curves for various values of ε_r

Table 1 Different values of ε_r

Electric permittivity	Absorption (%)	Frequency
4	95.8	10.42 GHz
4.1	95.8	10.3 GHz
4.2	95.8	10.15 GHz
4.3	95.8	10 GHz

tance when at the same time it can work as a multi- or broad-band absorber. Multi-band metamaterial absorbers can be implemented by properly scaling the original structure. Specifically, by multiplying the dimensions of the original S-ERR along the x- and y-axis by a scaling factor s, the center absorption frequency can be downshifted ($s > 1$) or up-shifted ($s < 1$), without changing the absorption curve's original shape and bandwidth. This property, frequently called metamaterial scalability property, will be, herein, used for the synthesis of multi-band absorbers. This feature can also be used to offer broad-band absorbers [14,15] by very slightly changing the scaling. Using this technique, it is possible to create multiple resonance bands and if the resonances are close enough in frequency to one another, to create a broad-band single peak. It is important to highlight that no scaling is applied along the z-direction, since the metal thickness has no effect on the behaviour of the absorbers. An example confirming the scalability feature for different scales of the original structure is presented in (Fig. 7; Table 2).

4 Dual-band absorption

Utilizing the conclusions drawn in the previous paragraph, we proceed in the design of a dual-band metamaterial absorber. Four electric resonators are imprinted at the front
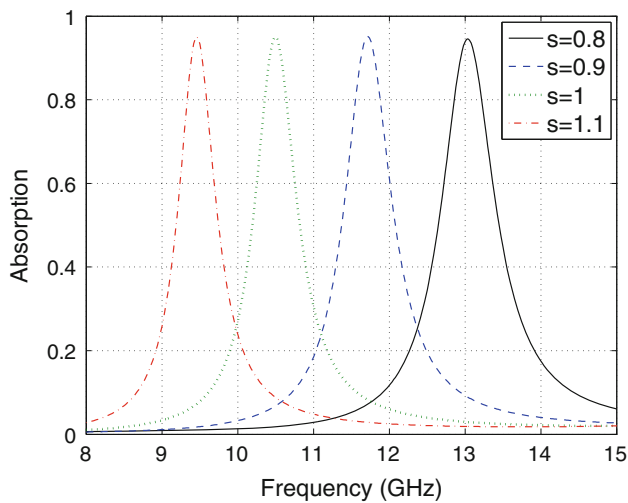
**Fig. 7** Absorption curves of the scaled versions of the proposed device

Table 2 Different scales of the ERR

Scales s	Absorption (%)	Frequency
0.80	95.8	13 GHz
0.90	95.8	11.7 GHz
1.00	95.8	10.3 GHz
1.10	95.8	9.46 GHz

face of a 1 mm thick FR-4 dielectric substrate, as in Fig. 8. The S-ERRs that are diagonally placed have the same dimensions. Two of them are scaled versions of the original S-ERR structure illustrated in Fig. 1a, with a scaling factor $s_2 = 0.90$, while the other two have the dimensions of the original ERR, and thus can be considered to be scaled by $s1 = 1.00$. The opposite side of the dielectric is covered by a full copper plane to guarantee zero transmission to enhance the absorption. From the results in [11], two distinct absorption peaks appear where the first occurs at 10.4 GHz, producing an almost perfect absorption of 99.3 %, while the second one occurs at 11.7 GHz and is reaching the value of 96 %. Furthermore, note that the absorption peak of the original S-ERR (in Fig. 1) is increased from 95.8 to 99.3 % in the dual-band structure showing that the addition of a second scaled S-ERR in the unit cell is slightly enhancing the structure's absorbing efficiency as well as offering another high absorption peak. Equally important to the multi-bandwidth performance of the absorber is proven to be its ability to absorb obliquely incident waves, even for large angles of incidence, which is newly presented in this paper. To this end, an analysis of the absorbing efficiency is held for two cases of oblique incidence (Fig. 9). Varying the angle θ, while retaining the angle $\varphi = 0.0$, results in very promising peak absorbances over 70 % up to a 60° angle at almost the same center frequencies as in the case of normal incidence. The absorbing efficiency deteriorates beyond that critical angle, yet remains at a 70 %
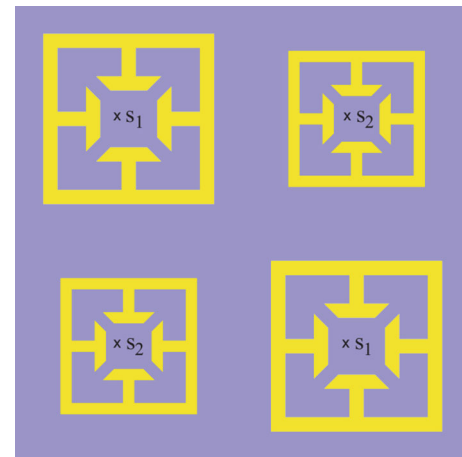
Fig. 8 Unit cell of a dual-band metamaterial absorber, consisting of four properly scaled S-ERRs where $s_1 = 1.00$ and $s_2 = 0.90$
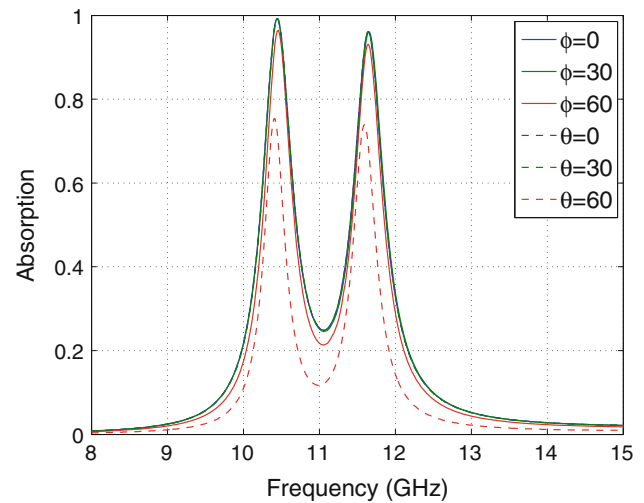

Fig. 9 Absorption efficiency of the dual-band absorber for obliquely incident waves in two different cases

peak for an incidence of 80° (omitted for clarity reasons). This deterioration phenomenon is attributed to the fact that the incident magnetic field can no longer efficiently drive circulating currents between the two metallic layers due to polarization since the magnitude of the incident magnetic component is reduced when angle θ increases (Fig. 5). On the other hand, for the variation of angle φ, the absorber's performance remains almost unchangeable and up to 99 and 96 %, respectively, verifying the wide-angle dual-band characteristic of the proposed structure (Table 3).

For various scaled versions of the S-ERR (where $\varphi = \theta = 0$), as shown in Fig. 10, the dual-band absorber exhibits high absorptive regions in different resonant frequencies. Observe the transition from dual-band absorption to broad-band, compared to the original S-ERR, in the cases where $s_1 = 1.00$ and $s_2 = 0.97$. Although two distinct peaks can be clearly identified in the resulting curve, the broad-band structure

Table 3 Various angles of incidence for the dual-band

Angle incidence	Degrees (°)	Peak 1 (%)	Peak 2 (%)
φ(phi)	0	99.3	96
φ	30	99.3	96
φ	60	99.3	96
θ(theta)	0	99.3	96
θ	30	96	93
θ	60	75	74
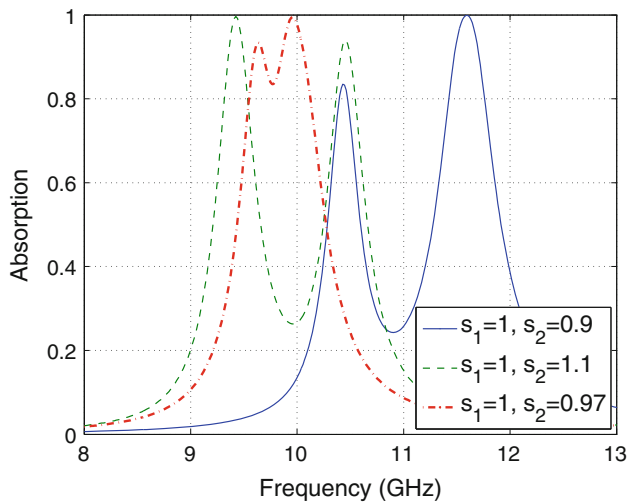
Fig. 10 Absorption curves of the scaled versions of the dual-band structure

Table 4 Dual-band absorber scaled variations

| s_1	s_2	Peak 1 (%)	Peak 2 (%)
1.00	0.90	99.3	96
1.00	1.10	99.5	94
1.00	0.97	93	99

absorbs over 85 % for twice the frequency band than the original structure (Fig. 1; Table 4).

5 Triple-band absorption

Following the design concept of the dual-band structure, we can easily move towards the construction of multi-band devices. A more complicated setup is the triple-band absorber, presented in Fig. 11. The unit cell design consists of a set of 3×3 S-ERR scaled elements. The scaling factors are $s_1 = 1.00$, $s_2 = 0.80$, and $s_3 = 0.70$ for the larger, medium, and smaller ERRs, respectively. From the simulation results in [11], we acquired three discrete absorption peaks. The first peak is an almost perfect 99.7 % at the frequency of 10.4 GHz, the second one approaches to 95.8 % absorption at 13 GHz, while the third one reaches a maxi-
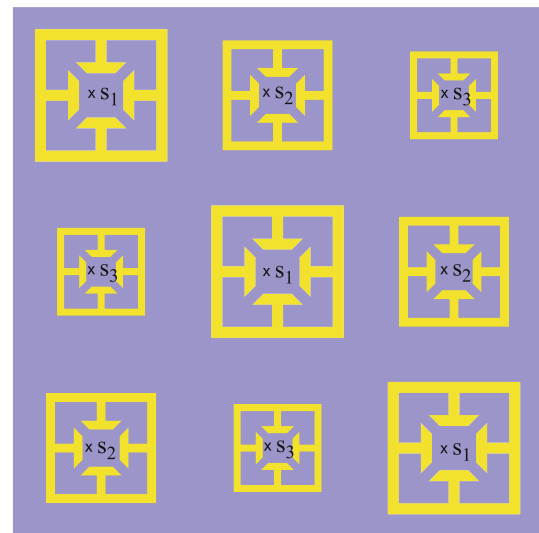
Fig. 11 Unit cell of a triple-band absorber, consisting of nine properly scaled ERRs. The dimensions of the bigger, medium, and smaller ERRs are those of Fig. 1 scaled by $s1 = 1$, $s2 = 0.8$ and $s3 = 0.7$, respectively
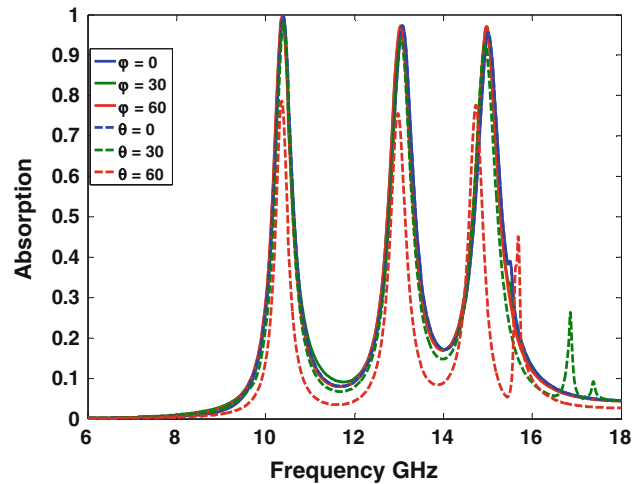
Fig. 12 Absorption efficiency of the triple-band absorber for obliquely incident waves in two different cases

mum of 95.5 %, at the frequency of 15 GHz. The shifts in the frequency zone can be viewed as a result of the coupling between the different S-ERRs since changing the scaling, the overall topology of the structure is affected. The wide angle performance is investigated also for the case of the triple-band absorber, proving the structures efficient operation for the various scenarios of oblique incidence. Firstly, we vary the angle theta which leads to high absorption rate over 75 % up to a 60° angle at almost the same center frequencies as in the case of normal incidence. Secondly varying the angle phi, we observe that the performance of the proposed triple-band structure remains almost unchangeable and up to 99 and 96 %, respectively, verifying the wide-angle triple-band feature of the absorber. It is also important to mention that the period of the supercell is relatively large and some weak

Table 5 Various angles of incidence triple band

Angle	Degrees (°)	A %	A %	A %
φ(phi)	0	99.7	97	96
φ	30	98.8	97	96
φ	60	98.8	96.6	97
θ(theta)	0	99.7	97	96
θ	30	98	94	92
θ	60	76	75	77

diffraction orders or waveguide modes may appear, specially at large illumination angles ($\theta \geq 60°$) (Fig. 12; Table 5).

Additionally, the surface current distributions at the three resonant frequencies are illustrated in Fig. 13. From this result, we can gain an insight into the physical mechanism of the absorption. At 10.4 GHz, surface currents indicate the resonant behaviour of the larger S-ERRs, while at 13 GHz the electric resonance of the medium S-ERRs is apparent. Finally, at 15 GHz, the smaller S-ERRs are responsible for the resonance. These outcomes suggest that the combination of unit cells with different absorbing frequencies can lead

to the superposition of their absorptive spectrum, confirming the idea for the creation of multi-band components.

6 Conclusions

A detailed example of multi-band absorption using a family of ultra-thin, polarization-insensitive, wide-angled metamaterial absorbers [11] that operate within the microwave spectrum has been presented. The physical mechanism behind the absorption of the basic structure has been explained. The proposed structures have been proven to exhibit several attractive characteristics by remaining electrically thin at the resonance frequency implementing a low-cost FR-4 dielectric substrate. By exploiting the geometrical scalability of the S-ERR elements, we have achieved multiple absorption peaks at the desired frequencies, thus extending our idea to dual-band and triple-band structures. Using this feature, these absorbers could be designed to work at other EM frequency range with nearly perfect absorption. Furthermore, the possibility to create broad-band absorbers was successfully exemplified using

Fig. 13 Surface current distributions on the front side of the triple-band absorber at *top left* 10.4 GHz, *top right* 13 GHz and *bottom left* 15 GHz. The lower absorption frequency is due to the resonance of the bigger ERRs, the intermediate peak corresponds to the resonance of the medium-sized ERRs while the higher one can be attributed to the resonant behaviour of the smaller ERRs
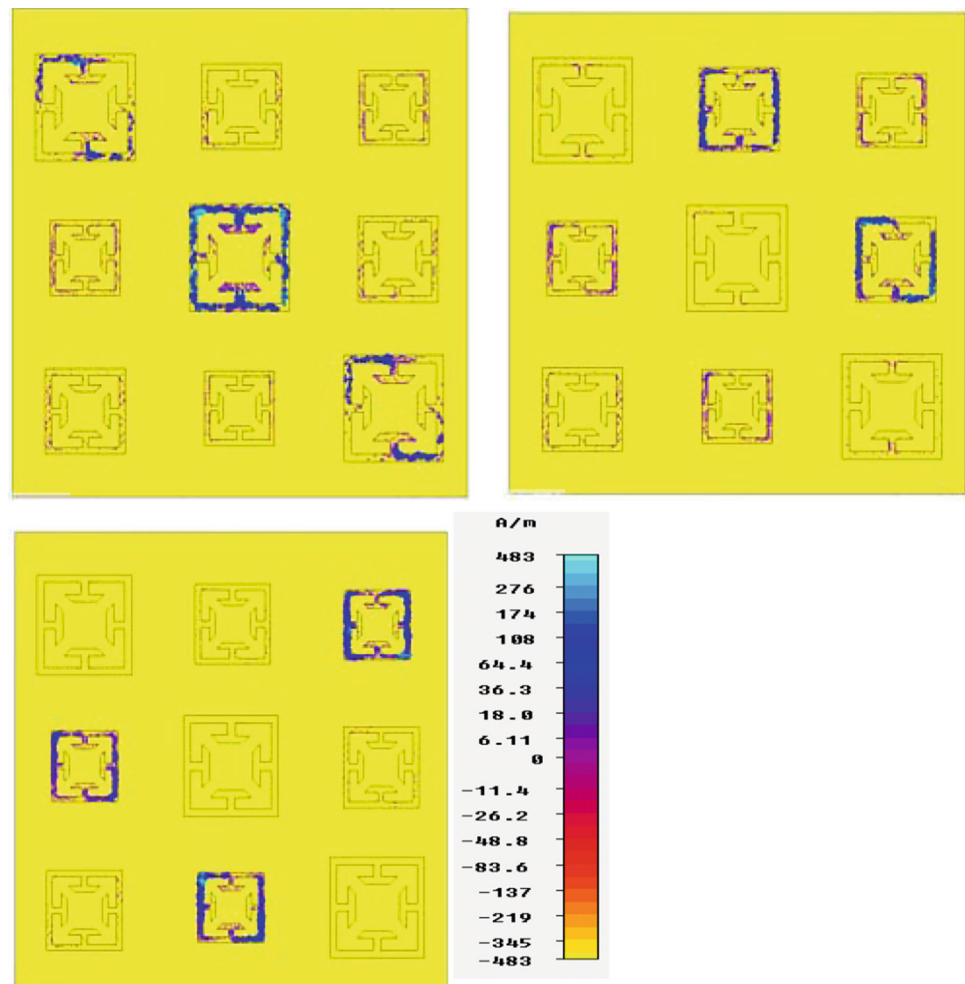
the dual-band arrangement with closely located resonances. The newly presented results from various incident angles constitute a strong indication for the angle-insensitive performance of the proposed multi-band absorbers. Finally, current distributions for the triple band structure verified our idea towards the realization of multi-band absorbers by combining unit cells with different absorbing frequencies. Such a composite microwave metamaterial may find numerous applications ranging from the active element in a bolometer to stealth technology. Future work will focus on the experimental verification of the acquired numerical results by measuring fabricated prototypes for the dual- and triple-band absorbers.

References

1. C. Watts, X. Liu, W. Padilla, Metamaterial electromagnetic wave absorbers. Adv. Opt. Mater. OP98–OP120 (2012)
2. C. Caloz, T. Itoh, *Electromagnetic Metamaterials: Transmission Line Theory and Microwave Applications: The Engineering Approach* (Wiley, New York, 2006)
3. R. Marqués, F. Martín, M. Sorolla, *Metamaterials with NegativeParameters: Theory, Design, and Microwave Applications* (Wiley, New York, 2008)
4. F. Bilotti, A. Toscano, K.B. Alici, E. Ozbay, L. Vegni, Design of miniaturized narrowband absorbers based on resonant-magnetic inclusions. IEEE Trans. Electromagn. Compat. **53**(63), 63–72 (2011)
5. W. Zhu, X. Zhao, B. Gong, L. Liu, B. Su, Optical metamaterial absorber based on leaf-shaped cells. Appl. Phys. A Mater. **102**(1), 147–151 (2011)
6. T. Kollatou, A. Dimitriadis, N. Kantartzis, M. Hinaje, C. Antonopoulos, A class of multi-band, polarization-insensitive, microwave metamaterial absorbers in EMC analysis. in *International Symposium on Electromagnetic Compatibility (EMC EUROPE)* (2012)
7. H. Tao, C. Bingham, A. Strikwerda, D. Pilon, D. Shrekenhamer, N. Landy, K. Fan, X. Zhang, W. Padila, R. Averitt, Highly flexible wide angle of incidence terahertz metamaterial absorber: design, fabrication and characterization. Phys. Rev. B **78**(24), 241103(1–4) (2008)
8. S. Xiaopeng, J.C. Tie, J. Zhao, H.F. Ma, W.X. Jiang, H. Li, Polarization-independent wide-angle triple-band metamaterial absorber. Opt. Express **19**(10), 9401–9407 (2011)
9. L. Huang, H. Chen, Multi-band and polarization insensitive metamaterial absorber. Prog. Electromagn. Res. **113**, 103–110 (2011)
10. Y.Z. Cheng, Y. Wang, Y. Nie, R.Z. Gong, X. Xiong, X. Wang, Design, fabrication and measurement of a broadband polarization-insensitive metamaterial absorber based on lumped elements. J. Appl. Phys. **111**(044902), 1–4 (2012)
11. T. Kollatou, A. Dimitriadis, S. Assimonis, N. Kantartzis, C. Antonopoulos, A family of ultra-thin, polarization-insensitive, multi-band, highly absorbing metamaterial structures. Prog. Electromagn. Res. **136**, 579–594 (2013)
12. H.T. Chen, J.F. O'Hara, A.J. Taylor, R.D. Averitt, C. Highstrete, M. Lee, W.J. Padilla, Complementary planar terahertz metamaterials. Opt. Express **15**, 1084–1095 (2007)
13. A. Taflove, S.C. Hagness, *Computational Electrodynamics* (Artech House, Boston, 2000)
14. S. Gu, J.P. Barrett, T.H. Hand, B.I. Popa, S.A. Cummer, A broadband low-reflection metamaterial absorber. J. Appl. Phys. **108**(064913), 1–6 (2010)
15. J. Sun, L. Liu, G. Dong, J. Zhou, An extremely broad band metamaterial absorber based on destructive interference. Opt. Express **19**(22), 21155–21162 (2011)